



ELSEVIER

Contents lists available at ScienceDirect

Optics Communications

journal homepage: www.elsevier.com/locate/optcom

Direct deconvolution of electric and magnetic responses of single nanoparticles by Fourier space surface plasmon resonance microscopy



C. Liu*, C.F. Chan, H.C. Ong

Department of Physics, The Chinese University of Hong Kong, Shatin, Hong Kong, People's Republic of China

ARTICLE INFO

Article history:

Received 15 March 2016

Received in revised form

18 May 2016

Accepted 22 May 2016

Available online 27 May 2016

Keywords:

Surface plasmons

Nanostructures

Optical imaging system

Near-field scattering

ABSTRACT

We use polarization-resolved surface plasmon resonance microscopy to image single dielectric nanoparticles. In real space, the nanoparticles exhibit V-shape diffraction patterns due to the interference between the incident surface plasmon polariton wave and the evanescent scattered waves, which arise from the interplay between the electric and magnetic dipoles of the nanoparticle. By using cross-polarized Fourier space imaging to extract only the scattered waves, we find the angular far-field intensity corresponds very well to the near-field scattering distribution, as confirmed by both analytical and numerical calculations. As a result, we directly deconvolute the contributions of electric and magnetic dipoles to the scattered fields without involving near-field techniques.

© 2016 Elsevier B.V. All rights reserved.

1. Introduction

Studying the interaction between surface plasmon polaritons (SPPs) and subwavelength entities has aroused much interest in science and engineering recently [1–6]. Notable examples include extraordinary transmission from nanohole arrays [4], trapping of nanoparticles by plasmonic tweezers [5], surface plasmon resonance (SPR) sensing [6], etc. In particular, SPR sensing has emerged as a major label-free biochemical technique in contrast to the fluorescence counterparts in which tagging is necessary for identification [6]. SPR spectroscopy and imaging detect the local change of refractive index upon the binding of target analytes to receptors for indicating their presence and thus no labels are required [7]. A minute change in refractive index is sufficient to be transduced into detectable optical signal, making SPR a high sensitive technique. Several types of SPR spectroscopic and imaging sensors based on spectral [8], angular [9] and phase [10] detections are now commercially available and each employs different plasmonic properties for detecting the refractive index change. However, they are all hinged on the conventional Kretschmann configuration where a prism coupler is necessary for exciting SPPs [8–10]. Prism-based imaging system suffers from low numerical aperture (NA) and magnification and it therefore does not provide good spatial resolution [11]. The best image resolution achieved so far is typically $\sim 3 \mu\text{m}$ for $\text{NA}=0.1$ at $\lambda=633 \text{ nm}$. Recently, Huang et al. attempts to overcome this obstacle by demonstrating an

objective-based SPR microscope in which a high NA and magnification objective lens is used to replace the prism coupler [12]. In analogy to total internal reflection fluorescence (TIRF) microscopy [13], a diffraction limited resolution is now possible in objective-based SPR microscope and features as small as $1 \mu\text{m}$ have been revealed evidently [14–16].

Recently, objective-based SPR microscopy has been used for imaging single subwavelength entity. For example, Tao and his coworkers have used this technique to image single Influenza A virus [14] and stretched DNA molecule [15]. Under SPP excitation, distinctive V-shape diffraction patterns are observed upon scattering of the incident plasmon wave by the molecules. Shan et al have further extended it to study the electrocatalytic activity of single metallic nanoparticles by simultaneously imaging and measuring their catalytic reactions [16]. Other than visible light, Halpern et al use near-infrared SPR microscope to real-time study DNA hybridization absorption in an in situ environment [17]. Although objective-based SPR microscopy shows great success in nanoscale imaging compared with its conventional SPR counterparts, a thorough understanding of how the shape, size, and material of the nanostructure affect the resulting image is of great importance. In principle, the geometry of the object governs the surface charge distributions, which create various electric and magnetic dipoles and subsequently determine the scattered fields [1,2]. Therefore, it is essential to differentiate the contributions of different dipoles to scattering and to understand their dependences on image formation. Several efforts on this issue have been seen lately. In particular, Fourier space, also known as momentum- or angle-resolved, imaging has become a powerful tool in quantifying the magnetic and electric dipole radiations [18].

* Corresponding author.

E-mail address: cliu@phy.cuhk.edu.hk (C. Liu).

Because of their differences in emission symmetry and polarization, it is possible to differentiate the contributions of electric and magnetic dipoles based on their angular emission and polarization patterns. Taminiou et al have distinguished the electric and magnetic dipole emissions from lanthanide ions by combining energy- and momentum-resolved spectroscopy [18]. Curto et al have studied the multipolar emissions from quantum dots attached to metallic nanoantennas [19]. On the other hand, Rotenberg et al have used near-field microscope to examine subwavelength nano-holes with different sizes [1,2]. They determine the corresponding electric and magnetic polarizabilities of the holes and the results agree well with analytical model.

In this work, we employ polarization-resolved real and Fourier space microscope to study the scattering of SPPs by dielectric silica nanoparticles. The SPR image exhibits typical V-shape diffraction pattern with long fan-like fringes pointing in the direction of SPP propagation due to the interference between the incident plane wave-like SPP and the evanescent scattered fields. Under cross-polarization, the incident background is removed to retrieve only the scattered fields. We find the angular far-field intensity distribution directly maps out the scattered near-field profile in Fourier space very well, as verified by analytical calculation and finite-difference time-domain (FDTD) simulations. Since the scattered fields evolve from the interaction between the in-plane magnetic and out-of-plane electric dipoles of the nanoparticle, we decouple them correspondingly.

2. Experimental method

The schematic setup of the SPR microscope is shown in Fig. 1(a). Briefly, an inverted microscope (Nikon Ti-U) equipped with a $100\times$, $NA=1.49$ oil-immersion TIRF objective lens is used to excite propagating SPPs on a 50 nm thick Au film deposited by magnetron sputtering on glass cover slip. The thickness of the film is confirmed by a stylus profilometer. A HeNe laser light at $\lambda=633$ nm emerging from a single mode fiber is first collimated by an achromatic lens and then is passed through a polarizer and a pellicle beam splitter before focused as a point source on the back focal plane of the objective lens. The light exiting from the objective lens thus evolves as a collimated beam illuminating on the sample at an incident angle θ defined as: $d = f \sin \theta$, where d is the offset of the point source from the optical axis of the objective lens and f is the focal length of the objective lens [12]. Therefore, by placing the illumination optics on a motorized linear translation stage with step size = $5 \mu\text{m}$, we vary the offset and thus the incident angle from 0° to 60° with angular

resolution down to 0.125° [20]. The radiation reflected from the sample is collected by the same objective lens and is then fed either into a photodiode for angular reflectivity measurement or CCD and EMCCD cameras for real and Fourier space imaging. For polarization-dependent measurements, an analyzer is placed in between the objective lens and the detection units. While the incident polarizer is always set at p-polarization with respect to the incident plane, the analyzer can be rotated. The angle between the polarizer and the analyzer is zero for parallel configuration but is 90° for orthogonal or cross-polarization. Two sizes of silica nanoparticles are purchased from Bang Laboratories, Inc. They are sonicated for 20 min before spin-coated on the Au films. In addition, prior to SPR imaging, all the samples are first examined by field-emission scanning electron microscope to confirm the size and shape of the nanoparticles. The inset of Fig. 1(b) shows that the nanoparticles have diameters $D=170$ and 310 nm, respectively, which both are smaller than the excitation wavelength.

We first demonstrate that our system is adequate for conducting objective-based SPR microscopy by showing the parallel and orthogonal angular plots of reflectivity of a flat Au film in Fig. 1(b). Apparently, from the parallel plot, a sharp reflection dip is visible at $\theta=43^\circ$, signifying the excitation of propagating SPPs on air/Au surface when the wavevector of the light source matches with that of SPPs. The plot is then compared with the simulation performed by WinSpall [21] and the calculation is plotted as the dash line in the figure. By assuming a three-layer glass/Au/air structure with Au thickness = 50 nm and the dielectric constants of glass (ϵ_g) and Au (ϵ_{Au}) = 2.31 and $-11.6 + 1.2i$, respectively, the calculation agrees with experiment. Slight discrepancy is noted due to surface roughness, thickness uncertainty, etc. On the other hand, the orthogonal plot shows much weaker signal (~ 200 times less than the parallel plot) as expected from the orthogonality between p- and s-polarizations. However, an asymmetric line-shape is found at the SPP resonant wavelength, indicating a very small p-to-s polarization conversion occurs due to the surface roughness. As pointed out by Crosbie et al. [22], when under SPR, surface roughness produces two s-polarized scattering channels which interfere with each other, resulting in the observed profile under orthogonal configuration. Nevertheless, both experiment and theory confirm the accuracy of the system.

3. Result

We then image the $D=310$ nm silica nanoparticle on Au film. We fix the incident angle at around 43° for exciting the Au/air

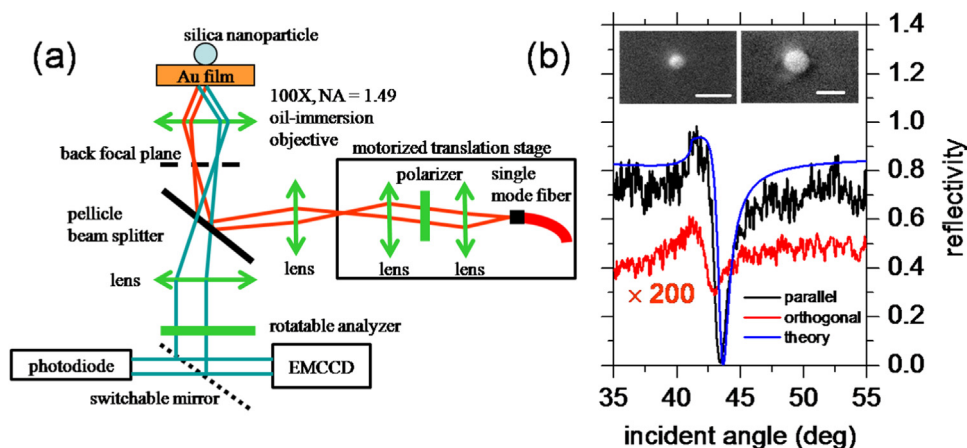


Fig. 1. (a) The schematic setup of SPR microscope. (b) The angular parallel (black line) and orthogonal (red line) reflectivity plots. The orthogonal plot is multiplied by 200 times for visualization. The theoretical curve is shown as the blue line. Inset: the scanning electron microscope images silica nanoparticle with $D=170$ and 300 nm. The scale bars are 350 nm. (For interpretation of the references to color in this figure legend, the reader is referred to the web version of this article.)

Download English Version:

<https://daneshyari.com/en/article/1533178>

Download Persian Version:

<https://daneshyari.com/article/1533178>

[Daneshyari.com](https://daneshyari.com)